Membrane Photopotential Generation by Interfacial Differences in the Turnover of a Photodynamic Reaction

Valerij S. Sokolov,* Michael Block,[†] Irina N. Stozhkova,* and Peter Pohl[†]

*Frumkin Institute of Electrochemistry RAS, Moscow, Russia, and [†]Institut für Medizinische Physik und Biophysik, Martin-Luther-Universität, 06097 Halle, Germany

ABSTRACT   The adsorption of a membrane-impermeable photosensitizer to only one membrane leaflet is found to trigger a localized photodynamic reaction; i.e., the amount of carbonyl cyanide m-chlorophenylhydrazone (CCCP) molecules damaged in the leaflet facing the photosensitizer is roughly identical to the total amount of CCCP inactivated. Whereas the latter quantity is assessed from the drop in membrane conductivity G, the former is evaluated from the photopotential φ that is proportional to the interfacial concentration difference of the uncoupler. Localized photodestruction is encountered by CCCP diffusion to the site of photodamage. A simple model that accounts for both photoinhibition and diffusion predicts the dependence of the photopotential on light intensity, buffer capacity, and pH of the medium. It is concluded that only a limited amount of the reactive oxygen species responsible for CCCP photodamage diffuses across the membrane. If the concentration of reactive oxygen species is decreased by addition of NaN_3 or by substituting aqueous oxygen for argon, φ is inhibited. If, in contrast, their life time is increased by substitution of H_2O for D_2O, φ increases.

INTRODUCTION

Photodynamic reactions are used for both diagnostics and treatment of cancer (Bachor et al., 1991; Canti et al., 1998; Diamond et al., 1972). The approach is based on the capability of photosensitizers (PS) to selectively accumulate in tumor cells and to initiate their damage upon exposure to visible light (Lee et al., 1995; Levy, 1994). The plasma membrane and the membranes of cellular organelles (mitochondria) have been found to be important sites of photodynamically induced cellular damage for most photosensitizers (Moore et al., 1997; Penning and Dubbelman, 1994). Conductivity changes are believed to be responsible for the vast majority of bioeffects mediated by photosensitizers with a tetrapyrrole ring structure. For example, a broad association was found between singlet oxygen quantum yield and clonogenic cell kill (Haylett et al., 1997). A hematoporphyrin-sensitized increase in membrane conductance and surface tension that is followed by membrane breakdown is observed upon light exposure of planar bilayer lipid membranes (BLMs) that are formed from unsaturated lipids. Photodynamically triggered lipid peroxidation does not occur when solely fully saturated lipids constitute the BLM (Stozhkova et al., 1992).

Aluminium-phthalocyanine was shown to mediate the photoinactivation of gramicidin due to the generation of reactive oxygen species (Rokitskaya et al., 1993). Singlet oxygen produced by photodynamic action causes inactivation of the mitochondrial permeability transition pore (Salet et al., 1997). The inactivation of membrane peptides may be also mediated by a photodynamic reaction of type I between a dye (Rose Bengal) and its tryptophan residues with a subsequent oxidation of the tryptophans (Kunz et al., 1995; Straessle and Stark, 1992). Generally, it is difficult to distinguish between both types of photodynamic reactions because not only phthalocyanines but a lot of other photosensitizers as well are able to induce both types of photodynamic reactions (Hoebeke et al., 1997; Rosenthal and Ben-Hur, 1995).

For a variety of sensitizers, the photosensitizing efficacy has been shown to correlate with their membrane association ability (Valenzeno and Tarr, 1991). In a study on model membranes, only the membrane-bound photosensitizer was found to contribute to gramicidin channel inactivation (Rokitskaya et al., 2000). Because the lability of membrane sites to photosensitization depends on the relative location of protein target and dye molecules (Kochevar et al., 1994), the question arises whether photosensitizer binding to only one membrane–water interface leads to an asymmetry of the photodynamic reaction between membrane leaflets. The lifetime of reactive oxygen species generated by a photosensitizer, in particular of singlet oxygen, is sufficient to allow transmembrane diffusion. Before reacting with a membrane-bound protein, encountering a quenching agent, or decaying from a variety of radiative and nonradiative processes, singlet oxygen lives about 3 μs in aqueous solution (Krasnovsky, 1998; Rodgers and Snowden, 1982) and 7 μs in lipid membranes (Ehrenberg et al., 1998; Krasnovsky, 1998). Because it can diffuse about 100 nm (Valenzeno and Tarr, 1991), an asymmetry in the turnover of the photodynamic reaction between membrane leaflets seems to be unlikely. However, differences in the diffusion velocity parallel and perpendicular to the membrane may confound this analysis.

Assuming different rates at which charged photoproducts are built at both membrane–water interfaces, the generation

---

of a photopotential is predicted. Photopotentials, in turn, are of great biological importance. For example, they must affect the open probability of voltage-dependent channels. A reduction of the open probability of membrane channels has already been observed (Kunz and Stark, 1998). The effect can be, in part, mediated by surface potential changes and by a simple decrease of the total number of membrane channels resulting from photodamage. Photopotentials have been observed in a channel-free system that contained the protonophore carbonylcyanide m-chlorophenylhydrazone (CCCP) and disodium anthraquinone-2,6-disulfonate. In the presence of the photosensitizer magnesium octaethylporphyrin, a photopotential was generated that pumped protons across a BLM. To explain the photoeffect, an interfacial pK_a-shift of CCCP was hypothesized to occur (Sun and Mauzerall, 1996).

As shown in the present work, preferential CCCP photodamage on only one of the two membrane–water interfaces represents an alternative explanation. The pronounced interleaflet asymmetry in the local rates of the photodynamic reaction was observed despite the fact that the reactive oxygen molecules responsible for the photoeffects are able to diffuse across the bilayer. Here it is shown that the total amount of CCCP inactivated is roughly identical to the amount of uncoupler molecules damaged in the leaflet facing the photosensitizer. Whereas the former quantity is assessed from the drop in membrane conductivity, G, the latter is evaluated from the photopotential φ. To predict φ, the diffusion of unmodified CCCP molecules to the site of photodamage was described by an analytical model.

THEORY

The following analysis is based on the assumption that photosensitizer adsorption to solely the *cis* membrane–water interface mediates a photodynamic reaction that is restricted to the same interface. The validity of the theoretical predictions is then proved in the experimental section.

In a monomolecular photodynamic reaction, the amount of CCCP molecules damaged is proportional to the aqueous CCCP concentration at the *cis* water–membrane interface c_c, the reaction rate k, and the local concentration of photoformed reactive oxygen species O_r:

$$J = kc_cO_r. \tag{1}$$

where k is considered to be equal for both the anion and the protonated forms of the weak acid. In the steady state, J (Eq. 1) is equal to the flow of unmodified CCCP molecules that occurs from the bulk to the site of the photodynamic reaction (Fig. 1). Transport occurs by diffusion because, even in vigorously stirred systems, there exists an unstirred water layer (USL) adjacent to planar membranes where convection is impossible. The protonophore flux consists of two parts:
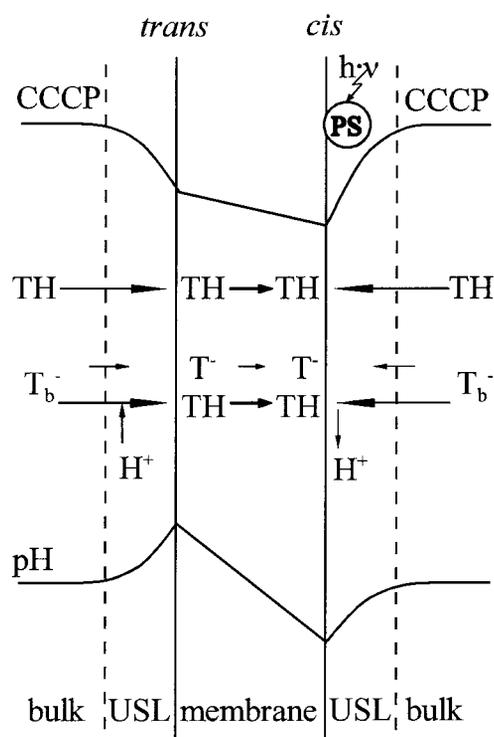

FIGURE 1 Photosensitizer (*PS*) adsorption to solely the *cis* membrane–water interface mediates a photodynamic reaction that preferentially takes place at the same interface. A flow of unmodified CCCP molecules is induced from the *cis* and *trans* bulk volumes to the site of the photodynamic reaction. Transport occurs by diffusion because, even in vigorously stirred systems, there exists an unstirred water layer (*USL*) adjacent to planar membranes where convection is impossible. Chemical reactions of proton uptake and release contribute to the transmembrane flux of the protonated CCCP molecules (*TH*). Their membrane permeability is much higher than the permeability of the CCCP anion (T_-). In a medium with a low buffer capacity, a pH gradient develops within both USLs.

1. The flux J_c from the *cis* bulk solution to the *cis* interface,

$$J_c = P_{UL}(c_b - c_c) = P_{UL}\Delta c, \tag{2}$$

where P_{UL}, c_b and c_c are, respectively, the permeability of the USL, the concentration of the protonophore in the bulk, and at the *cis* membrane–water interface. Δc is the decrease of CCCP concentration due to photodamage.

2. The flux J_t that is equal to the flux $J_{USL,\,t}$ across the *trans* USL and to the flux J_M across the membrane,

$$J_{USL,t} = P_{UL}(c_b - c_t), \tag{3}$$

$$J_M = P_M(TH_t - TH_c), \tag{4}$$

where TH_t, TH_c and P_M are, respectively, the *trans* and *cis* interfacial concentrations of the undissociated weak acid and their membrane permeability. The transmembrane flux of the CCCP anion is neglected because its membrane permeability is much smaller (2×10^{-3} cm/s) than the one of the undissociated molecule (11 cm/s) (LeBlanc, 1971).

Furthermore, under open circuited conditions, the total transmembrane electric current is equal to zero, and, hence, there is no net flux of the anionic form of CCCP across the membrane. Eqs. 1, 3, and 4 can be combined into

$$\frac{J_{USL,t}}{P_{UL}(\alpha + 1)} + \frac{J_M}{P_M\alpha} + \frac{J}{kO_r(\alpha + 1)} = T_b^-, \quad (5)$$

where T_b^- is the bulk concentration of the protonophore anion. For small interfacial pH gradients, the ratio α of the concentrations of the protonated and charged CCCP molecules is a constant, i.e., it does not depend on the distance to the membrane. The USL-permeability, P_{UL}, is equal to 3×10^{-4} cm/s, i.e., it is more than four orders of magnitude smaller than P_M. P_{UL} was calculated as the ratio of the diffusion coefficient D (4.5×10^{-6} cm^2/s as estimated from the molecular weight) and the USL thickness, δ (according to microelectrode measurements (Pohl et al., 1998) about 150 μm). Because the pK_a of CCCP is equal to 6.1 (Le-Blanc, 1971), $\alpha > 10^{-3}$ in the pH interval from 5 to 9. With respect to $J_{USL,t} = J_M = J_t$, Eq. 5 can be simplified:

$$\frac{J_t}{P_{UL}(\alpha + 1)} + \frac{J}{kO_r(\alpha + 1)} = T_b^-. \quad (6)$$

A similar expression for J_c is derived from Eqs. 1 and 2. Consequently, J_t and J_c are equal to each other:

$$J = 2J_t = 2J_c. \quad (7)$$

Eq. 6 is simplified with the help of Eq. 7:

$$\frac{1}{J} = \frac{1}{2P_{UL}c_b} + \frac{1}{kO_rc_b}. \quad (8)$$

As in the case of any other weak acid, chemical reactions of proton uptake and release by CCCP contribute to its transmembrane flux (Gutknecht and Tosteson, 1973). J_t can be considered as the sum of the fluxes J_{TH} and J_{T-} (Antonenko and Yaguzhinsky, 1982):

1. J_{TH} is determined by the flux of the neutral acid through the *trans* USL, through the membrane, and by its subsequent photodamage (derived in close analogy to Eq. 8),

$$\frac{J_{TH}}{2P_{UL}} + \frac{J_{TH}}{kO_r} = TH_1. \quad (9)$$

2. The flux J_{T-} of the acid anion is found from Eqs. 8 and 9 as

$$J_{T^-} = J_t - J_{TH} = \frac{2P_{UL}kO_rT_b^-}{2P_{UL} + kO_r}. \quad (10)$$

Unlike J_{TH}, the flux J_{T-} produces a pH shift in the USLs. In the presence of a protonophore, the pH-gradient gives rise to a Nernstian transmembrane potential n that can be used to assess J_{T-} (Antonenko and Yaguzhinsky, 1982). In the steady state, the flux J_{T-} must be equal to the oppositely

directed buffer flux, J_b across both the *cis* and *trans* USL (Pohl et al., 1993):

$$J_{T^-} = J_b = \frac{bP_{UL}\Delta pH}{2} = \frac{bFD_b\varphi}{4.6RT\delta}. \quad (11)$$

Eqs. 10 and 11 can be combined as

$$\varphi = \frac{4.6RTkO_rT_b^-}{Fb(2P_{UL} + kO_r)}. \quad (12)$$

According to Eq. 12, the membrane potential can be used to evaluate the turnover of the photodynamic reaction. n reflects exclusively the flux arising from interfacial differences in the amount of protonophore damaged.

J can be also assessed from the photoinduced decrease in membrane conductance, ΔG, because the protonophore concentration is proportional to the membrane conductivity (at least at low CCCP concentrations). The steady-state conductivity during illumination, G_{light}, is determined by the initial dark conductivity, G_{dark}, and by the rate of protonophore depletion inside the membrane due to photodamage. The latter is encountered by backdiffusion of intact protonophore molecules from the aqueous bulk solution across both USLs. With respect to the great membrane permeability of CCCP, its transmembrane concentration difference is small compared to Δc, no matter where the photodamage takes place—solely at the *cis* or at both interfaces. From Eqs. 2, it follows that

$$J = \frac{2D}{\delta}\Delta c. \quad (13)$$

In the following, it will be convenient to use the relative conductivity changes G_{rel},

$$G_{rel} = \frac{G_{dark} - G_{light}}{G_{light}} = \frac{\Delta G}{G_{light}} = \frac{\Delta c}{c_b - \Delta c}. \quad (14)$$

Fom Eqs. 1, 13, and 14, G_{rel} can be expressed as

$$G_{rel} = \frac{\delta}{2D}kO_r. \quad (15)$$

It is assumed that the photoproducts do not significantly contribute to the total conductivity. The photoeffect depicted in terms of G_{rel} does not depend on the CCCP concentration in aqueous solution. Finally, a combination of Eqs. 13 and 14 allows calculation of J from the decrease in relative membrane conductance G_{rel},

$$J = \frac{2P_{UL}G_{rel}c_b}{1 + G_{rel}}. \quad (16)$$

Eq. 16 returns the total CCCP flux induced by its photodamage. In contrast to Eq. 12, it reflects not the interleaflet difference in the number of damaged uncoupler molecules but their sum. A comparison of J and J_t allows proof of the

initial assumption about the interfacial differences in the rates of the photodynamical reaction.

MATERIALS AND METHODS

Planar bilayer lipid membranes were formed by a conventional method (Mueller et al., 1963) in a hole, 1.0 mm in diameter, on a diaphragm dividing a polytetrafluorethylene chamber. The membrane-forming solutions contained 15 mg diphytanoyl-phosphatidyl-choline (Avanti Polar Lipids, Alabaster, AL) per ml n-decane (Merck, Darmstadt, Germany). The solutions surrounding membrane were agitated by magnetic bars. They were prepared in deionized water from NaCl and KCl (all Merck) in different concentrations and buffered with 3-[cyclohexylamino]-2-hydroxy-1-propanesulfonic acid (CAPSO) (Fluka, Buchs, Switzerland) or morpholinoethanesulfonic acid (Boehringer, Mannheim, Germany) or NaH_2PO_4 (Merck). CCCP (Fluka) and tetrachlorotrifluoromethylbenzimidazole (TTFB) were added from ethanol stock solutions to the aqueous phase at both sides of the membrane. The total ethanol concentration did not exceed 1%. The photosensitizer chloroaluminum phthalocyanine tetrasulfonate ($AlPcS_4$) (Porphyrin Products, Logan, UT) was given to the *cis* compartment of the cell from concentrated aqueous solutions.

The membranes were exposed to monochromatic light (670 nm) from a 1-kW xenon-lamp (Oriel Instruments, Stratford, CT). The slits of the monochromator were set to a bandwidth of 20–40 nm. To measure the intensity of the focused monochromatic light beam, the membrane was replaced by a total absorber (model RTN-31C, VNIIOFI, Moscow, Russia). At a wavelength of 670 nm, the output of the attached calibrated thermoelement was equivalent to an intensity of 20 W/m². A definite decrease in the intensity of the light was achieved by neutral glass filters (Edmund Scientific, Barrington, NJ).

To measure conductivity and capacitance of the BLM, an alternating triangular input wave with an amplitude of ∼10–30 mV was applied via a silver/silver-chloride electrode and an agar bridge to the aqueous phase at one side of the membrane. The output signal from a second electrode at the opposite side of the membrane was amplified by a picoampermeter (model 428, Keithley Instruments, Cleveland, OH), digitized by an oscilloscope (model TDS 340, Tektronix Inc., Wilsonville, OR) and continuously visualized as a function of the input voltage by a personal computer. Membrane capacitance was calculated as a function of the area occupied by the resulting parallelogram, whereas the conductivity was obtained from the slope of current–voltage curve at zero input voltage. To measure the transmembrane potential, an impedance converter (AD546, Analog Devices, Norwood, MA) was used. With respect to the known frequency dependence of the CCCP- or TTFB-mediated membrane conductance (Borisova et al., 1974; Kasianowicz et al., 1984), the frequency of the
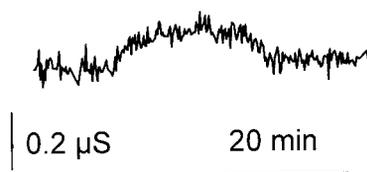
applied voltage was fixed between 1 and 10 Hz for CCCP and between 60 and 100 Hz for TTFB. In this range, the BLM conductivity varies little with frequency.

RESULTS

The conductivity of the pure lipid bilayer (8 ± 2 nS cm^{-2}) was neither affected by $AlPcS_4$ addition nor by subsequent illumination. Consequently, it is assumed that neither the PS itself nor any of its photoproducts was able to damage the lipid matrix. This observation is in agreement with earlier reports where BLMs formed exclusively from fully saturated lipid were described to be an excellent tool for the investigation of photoeffects on membrane transport systems because lipid oxidation processes do not interfere (Stozhkova et al., 1997). The dark conductivity, G_{dark}, of BLMs doped with TTFB was not distinguishable from the conductivity measured during light exposure. The only effect mediated by the $AlPcS_4$ was an increase in light-energy absorption so that intense and prolonged illuminations led to
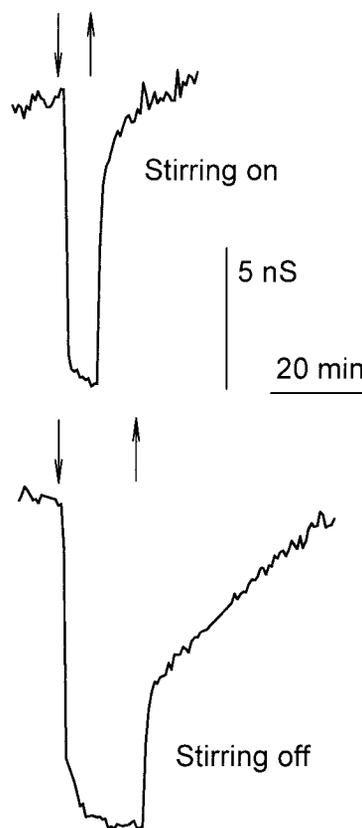
FIGURE 3 Typical experimental record showing the photoinhibition of CCCP-mediated membrane conductivity. The solutions contained 100 mM KCl, 1 mM NaH_2PO_4, and 1 μM CCCP. pH was 7.0. $AlPcS_4$, 14 μM, was given to the *cis* side only. At the time marked by downward and upward arrows, the monochromatic light source that was placed at the *trans* side of the membrane was switched on and off, respectively. The photoeffect observed in (*A*) a well-stirred chamber differs from the one obtained (*B*) under unstirred conditions.

FIGURE 2 Lack of photosensitizing activity of aluminum phthalocyanine tetrasulfonate ($AlPcS_4$, 14 μM in the *cis* compartment) on TTFB-mediated membrane conductivity. An alternating voltage with a peak to peak amplitude of 10 mV was applied at a frequency of 60 Hz. The buffer solutions contained 100 mM KCl, 1 mM NaH_2PO_4, and 0.5 μM TTFB. pH was 7.0. Long-term illumination with monochromatic light (670 nm) lead to an increase in the temperature (1 K) of the buffer solutions that was accompanied by a modest increase in conductivity. In the dark, the transmembrane current decayed to baseline.
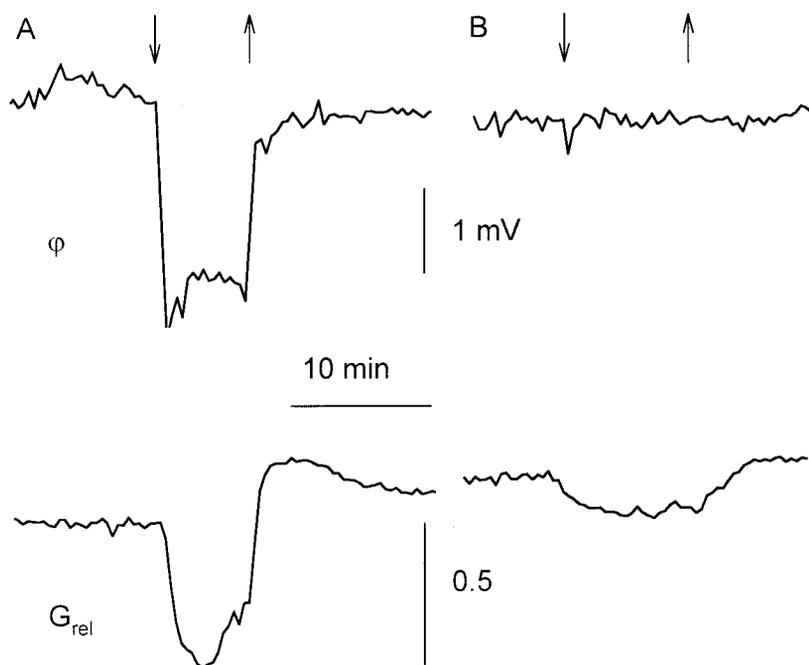
FIGURE 4 Inhibitory effect of 10 mM sodium azide on photopotential and light-driven changes of membrane conductivity. The *cis* compartment held 15 μM AlPcS$_4$. The aqueous solution (pH 9.0) consisted of 100 mM KCl, 16 μM CCCP, and 1mM CAPSO.

a moderate heating of the solutions surrounding the membrane. The latter than transformed into a small and slow augmentation of membrane conductivity (Fig. 2).

A completely different picture was observed when CCCP was substituted for TTFB. Light exposure resulted in a fast decrease of membrane conductivity that depended on Al-PcS$_4$ or CCCP concentrations and light intensity. The light-driven effects correlated with the absorption spectrum of phthalocyanine. They were most pronounced at a wavelength of 670 nm corresponding to the adsorption peak. At low concentrations of the protonophore (up to 10 μM), the photoeffect was reversible. In the dark, the initial membrane conductivity was completely restored, i.e., there was no difference between the initial and the steady-state conductance measured after light exposure (Fig. 3 A). The relaxation time depended on the rate at which the buffer solutions surrounding the membrane were stirred. The higher the stirring rate was, the faster membrane conductivity returned to the baseline (Fig. 3, A and B). From the stirring effect, it was concluded that transport processes across the USL were involved. Rigorous stirring diminished the thickness, δ, of this diffusional barrier and accelerated the substitution of damaged CCCP-molecules for intact molecules from the aqueous phase. The photoinduced decrease in conductivity depended also on the stirring conditions (Fig. 3). The larger the USL, the more pronounced was the photoeffect because intact protonophore molecules encountered a higher resistance to enter the membrane.

CCCP-photodamage is likely to be mediated by reactive oxygen species because various phthalocyanine derivatives of phototherapeutic interest have been shown to be efficient

type II (singlet oxygen, $^1O_2$) sensitizers in aqueous and nonaqueous solutions (Lagorio et al., 1989; Rokitskaya et al., 1993). In our system, the addition of azide inhibited the photopotential (Fig. 4). However, membrane conductivity was only partly prevented from being modified by illumination. These observations do not necessarily contradict each other because azide can intercept any $^1O_2$ escaping into

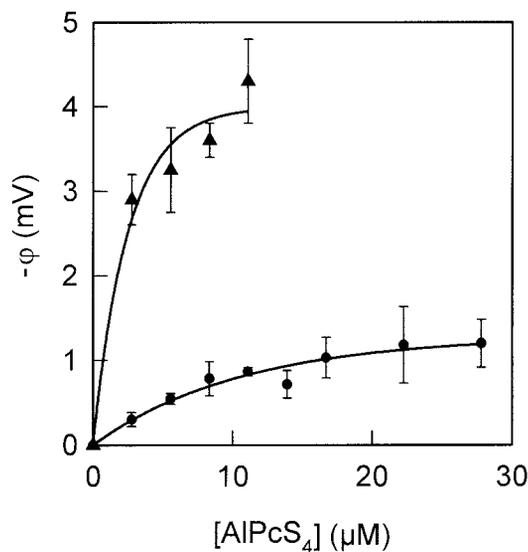FIGURE 5 Dependence of photopotential on the concentration of Al-PcS4. The buffer solutions (pH 6.7) consisted of 100 mM KCl, 1 mM KH$_2$PO$_4$, 38 μM CCCP. The *cis* compartment held 11 μM AlPcS$_4$. Substitution of H$_2$O (*circles*) for D$_2$O (*triangles*) leads to an increase of the photopotential.

FIGURE 6 A decrease of the aqueous oxygen concentration by bubbling the solutions with Argon diminished the photopotential. The bulk solution contained 100 mM KCl, 1 mM KH_2PO_4 and 38 μM CCCP at pH 6.7 in (A, B) water or (C, D) heavy water. $AlPcS_4$, 11 μM, was added to the *cis* side of the membrane.
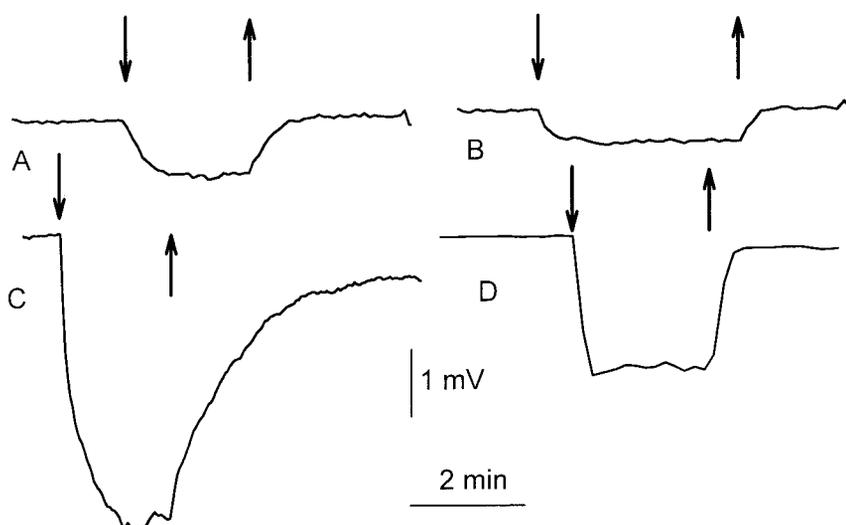
(or formed in) the medium, however, it has limited access to $^1O_2$ generated on the membrane and reacting (or being quenched) near its site of origin (Bachowski et al., 1991).

Experiments carried out in D_2O solutions provided additional support for protonophore destruction by reactive oxygen species. With the removal of hydrogen bonds between the water molecules that are known to serve as natural scavengers of singlet oxygen (Rywkin et al., 1992; Zang et al., 1995), the light-driven changes in membrane potential and conductivity were predicted to increase. As seen from Fig. 5, the experimental results are in agreement with this anticipation. Furthermore, the substitution of aqueous oxygen for argon that was achieved by the translation of argon bubbles through the buffer solutions, also reduced the photopotential (Fig. 6). Again, when H_2O was substituted for D_2O, bubbling of the buffer solutions with argon led to a decrease of the membrane potential (Fig. 6).

According to the model derived in the theoretical section, the membrane potential is predicted to depend on buffer capacity. In agreement with Eq. 12, φ diminished with increasing b (Fig. 7). At the same time G_{rel} remained unchanged because the amount of CCCP molecules damaged does not depend on b (Fig. 7).

In agreement with the model, Fig. 8 A shows a negligible dependence of G_{rel} on the aqueous protonophore concentration up to 10 μM CCCP (Eq. 13). This is exactly the concentration range G_{dark} changes linearly with the CCCP concentration, c_b (Fig. 9). In the same concentration range, a photopotential, n, was generated (Fig. 8 B). According to the model, the fluxes J_t and J were calculated from n (Eq. 11) and G_{rel} (Eq. 16), respectively (Fig. 8 C). The buffer capacity required for the calculation of J_t is found from the value of the equilibrium constant K_a of the buffer and the buffer (c_{buffer}) and proton concentrations,

$$b = \frac{2.3 K_a [H^+]}{(K_a + [H^+])^2} c_{buffer}. \tag{17}$$

With respect to the surface potential introduced by $AlPcS_4$ adsorption (Rokitskaya et al., 2000), the concentration of charged buffer species adjacent to the membrane is further reduced. Assuming a Boltzman distribution, b was found to be of 0.2 mM under the conditions shown in Fig. 8.

For the case that CCCP photodamage takes place exclusively at the PS-containing membrane–water interface, J_t was predicted to be equal to $J/2$ (Eq. 7). If the photodynamic reaction proceeds on both interfaces, the difference in the interfacial CCCP concentrations, and hence J_t, is expected to be smaller. According to Fig. 8 C, however, J_t is as large as J. Because the USL permeability for buffer diffusion equals ($D/\delta = 4.5 \times 10^{-6}$ cm^{-2} s^{-1}/0.015 cm) 3×10^{-4} cm/s, a buffer flux of 3 nM cm^{-2} s^{-1} (Fig. 8) corresponds to a gradient of the effective buffer concentration of 10^{-5} M ($J_b = P_{UL} \times \Delta b$), i.e., the buffer capacities adjacent to the membrane and in the bulk differ by a factor of two. When J_t is corrected for the lower buffer capacity, the prediction of Eq. 7 is found to be fulfilled, i.e., J_t approximately equals $J/2$. It is concluded that CCCP photodamage occurs preferentially on the membrane leaflet facing the PS.

For a CCCP concentration interval, where G_{dark} is proportional to c_b (Fig. 9), Eqs. 15 and 12 describe, respectively, G_{rel} and n as linear functions kO_r, i.e., of light intensity, I. The experiment confirmed the prediction (Fig. 10, A and B). When calculated from φ and G_{rel}, J_t is equal to J (Fig. 10 C). If, in analogy to Fig. 8, the near-membrane buffer depletion is taken into account, J_t diminishes by a factor of two. Again, Eq. 7 is found to be satisfied.

Also the pH dependence of φ is properly described by the model. Because φ is a measure of J_{T-} (Eq. 11), it is expected to increase with an increase in the concentration of the CCCP anion, e.g., with an augmentation of pH. In agreement with the model, φ reached saturation when all protonophore molecules were deprotonotated at pH $\gg$ pK_{CCCP} (Fig. 11 A). G_{rel}, on contrary, should not depend on pH, as was confirmed by the experiment (Fig. 11 B).
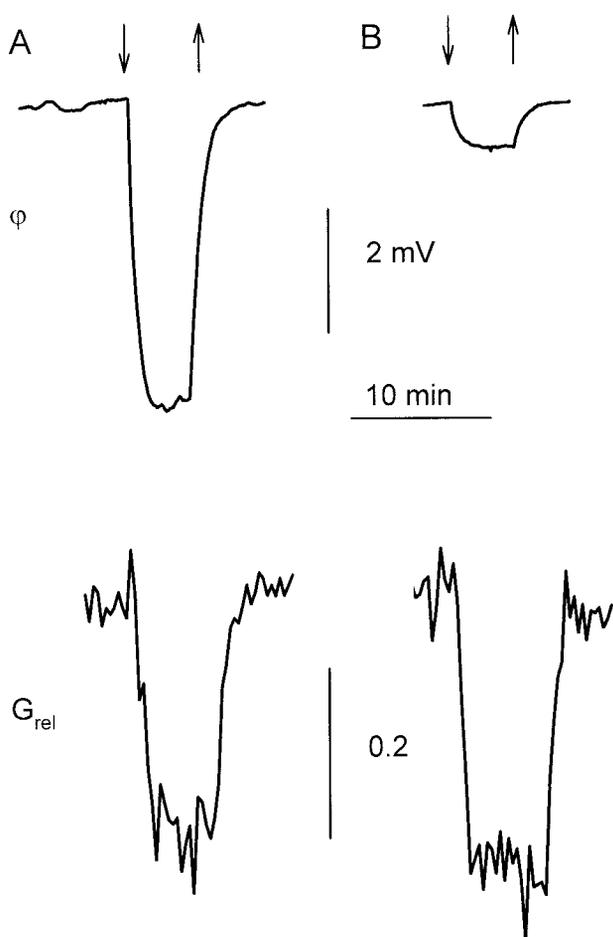
FIGURE 7 The effect of buffer capacity on light-driven changes of potential and conductivity. The *cis* compartment held 15 μM AlPcS$_4$. Aqueous solution (pH 9.0) consisted of 100 mM KCl, 7.4 μM CCCP, and (*A*) 1mM CAPSO or (*B*) 5mM CAPSO. Light exposure was limited to the time between the arrows.

Deviations from the theory were observed at high CCCP concentrations ($>$10 μM). They were contributed to a considerable amount of photoproducts. Their accumulation resulted in a monotonous increase of G_{light} and membrane rupture (Fig. 12 *A*). Aborting light exposure before membrane breakdown revealed an irreversible augmentation of conductivity (Fig. 12 *B*). In the dark, some additional conductivity that was not mediated by intact CCCP molecules always retained. A representative experimental record is shown for an intermediate CCCP concentration (Fig. 12 *C*). Here, a superposition of both types of kinetics was observed: an initial reversible conductivity drop caused by illumination was followed by a subsequent slow and irreversible increase in conductivity. The time course of conductivity changes was very sensitive to light intensity. The lower the light intensity, the more the system approached the borderline kinetics shown in Fig. 3 *A*, whereas at very high intensities, pictures similar to the one demonstrated in Fig. 12 *A* were obtained.
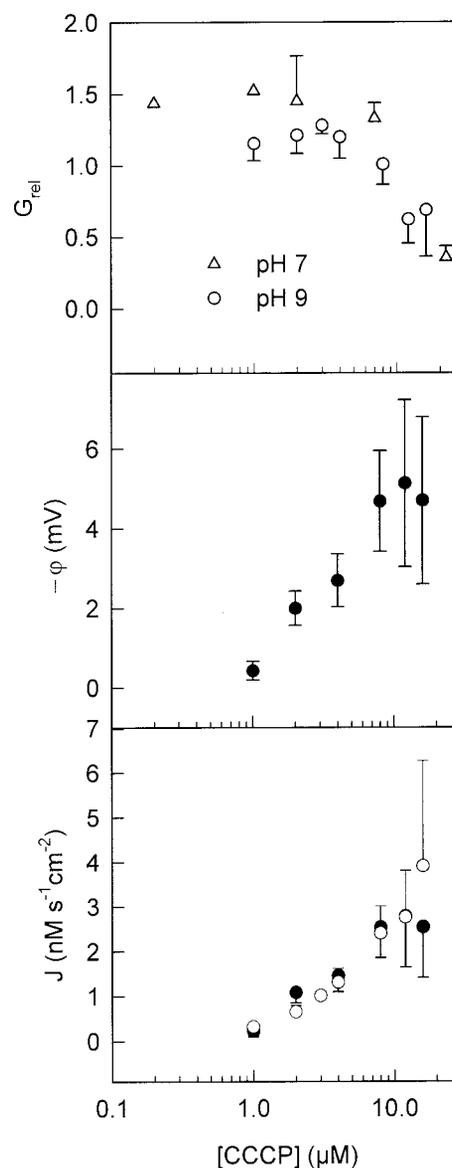

FIGURE 8 Light-driven changes of (*A*) relative conductivity and (*B*) membrane potential as a function of the aqueous CCCP concentration. The *cis* aqueous solution contained 14 μM AlPcS$_4$. Circles and triangles correspond to measurements carried out in 100 mM KCl, 1 mM KH$_2$PO$_4$ at pH 7.0 and 100 mM KCl, 1 mM CAPSO, pH 9.0, respectively. (*C*) According to Eqs. 11 and 16, the fluxes J_t and J were calculated from φ and G_{rel}.

DISCUSSION

Exposure to light induces a membrane potential and changes of membrane conductance when the photosensitizer AlPcS$_4$ is adsorbed to one leafleat of a protonophore (CCCP)-containing planar bilayer. The photoeffects are generated by photodynamic damage of CCCP. Strong support for this conclusion comes from experiments in which membrane conductivity and potential changes were found to be promoted or inhibited by quenching or enhancing agents
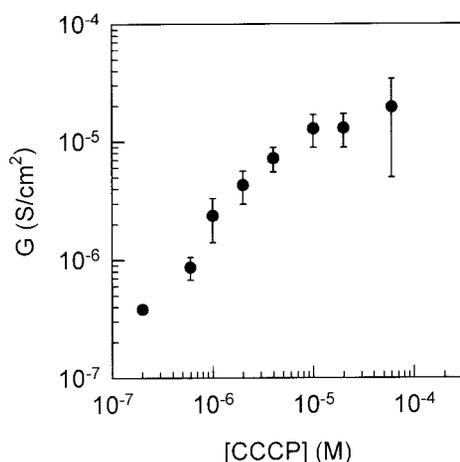
FIGURE 9 Membrane dark conductivity as a function of CCCP buffer concentration. The conditions were similar to the experiments shown in Fig. 3.

of reactive forms of oxygen (Figs. 4–6). Unfortunately, neither the inhibition of the photoeffect by sodium azide nor the increase of the photopotential in D_2O, in which singlet oxygen has a longer lifetime than in H_2O, are completely specific for singlet oxygen. Photoinduced electron abstraction from chemical additives was suggested to be a likely source of one electron-oxidized primary radical, which can provide the precursors of the oxidative damage in phthalocyanine photosensitization (Rosenthal and Ben-Hur, 1995). Although, the presence of molecular oxygen is a determinant in the photoeffect of $AlPcS_4$ in our system (compare Figs. 5 and 6), and photosensitized oxidation is the accepted chemical mechanism for its photodynamic action, it is difficult to establish whether the process is initiated by a type I electron transfer, or by a type II energy transfer reaction to form singlet oxygen.

Previously, light-driven potential and current changes across planar bilayers doped with CCCP have also been observed in a system containing magnesium octaethylporphyrin and disodium anthraquinone-2,6-disulfonate (Sun and Mauzerall, 1996). The authors suggested that it is an interfacial pK_a shift of CCCP caused by the local electric field of photoformed porphyrin cations/acceptor anions that functions as the driving force for the proton-pumping effect. An increase in proton pumping observed when H_2O was substituted for D_2O was interpreted in terms of a decreased ionization of CCCP (Sun and Mauzerall, 1996). Nevertheless, a concomitant increase in the lifetime of reactive oxygen species (Chou and Khan, 1983; Rywkin et al., 1992; Zang et al., 1995) that are known to be generated by a variety of PS (Levy, 1994; Penning and Dubbelman, 1994; Prinsze et al., 1990) provides an alternative explanation for the photopotentials and photocurrents observed. Moreover, we have recorded similar photoeffects also in the absence of an electron acceptor in our experiments. The photoeffects
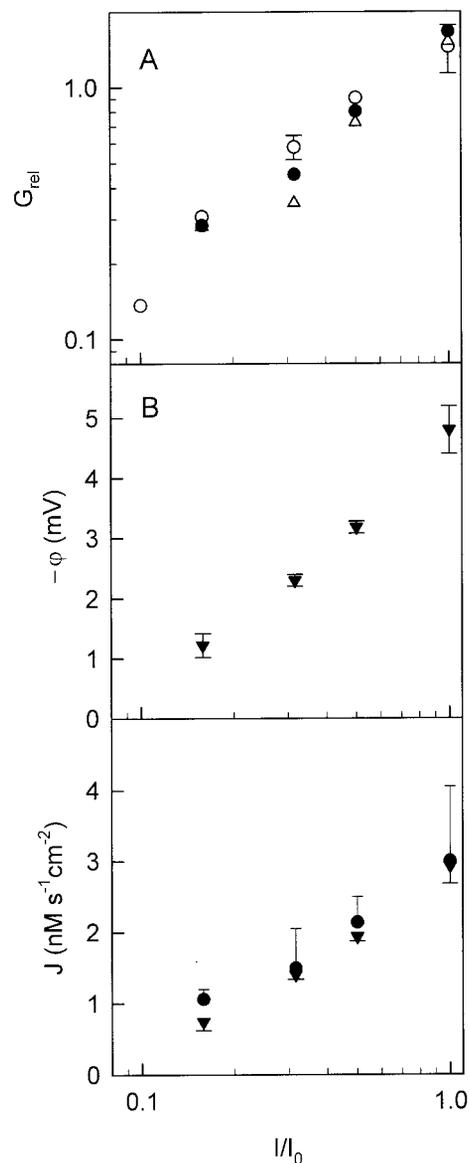
FIGURE 10 Light-driven changes of (A) relative conductivity and (B) membrane potential as a function of relative light intensity. By using neutral density filters, the initial light intensity, I_0, was diminished to the intensity, I. Measurements were carried out in the presence of 1 μM (*triangles*), 4 μM (*inverted triangles*) and 7.8 μM (*circles*) CCCP. The *cis* compartment held 14 μM $AlPcS_4$. Hollow and filled symbols designate results obtained with buffer solutions containing 100 mM KCl, 1 mM KH_2PO_4 (pH 6.7) or 100 mM KCl, 1 mM CAPSO (pH 9.0), respectively. (C) According to Eqs. 11 and 16, the fluxes J_t and J were calculated from φ and G_{rel}.

occurred in the presence of CCCP but not in a system containing TTFB. Hence, it is not the difference in the sensitivity to the local electrical field but rather the incapability of TTFB to experience a photodynamic reaction that is responsible for the divergence observed between the uncouplers.

Consequently, the mechanism of $AlPcS_4$-sensitized photopotentials and conductance changes, i.e., CCCP photoin-
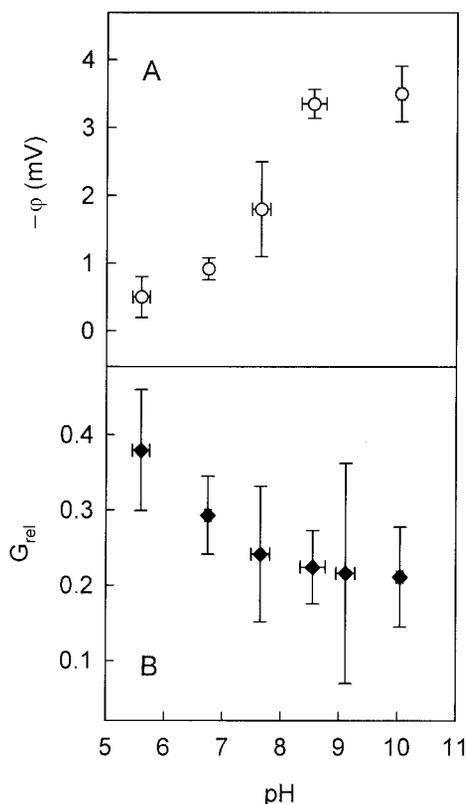
FIGURE 11 Light-driven changes of (A) relative conductivity and (B) transmembrane potential as a function of pH of the buffer solutions (100 mM KCl, 1 mM CAPSO, 1 mM KH_2PO_4, 7.7 μM CCCP). The *cis* compartment held 15 μM AlPcS$_4$.

activation is similar to the one that leads to the photoinhibition of model channels (Kunz et al., 1995; Rokitskaya et al., 1993), to lipid peroxidation (Bachowski et al., 1991; Girotti, 1990), and apoptosis (Ahmad et al., 1998; He et al., 1998).

AlPcS$_4$ is able to sensitize an increase in membrane conductivity as well as its decrease. The direction of the photoeffect depends on the protonophore concentration: G_{light} is smaller than G_{dark} at low protonophore concentrations. Their relation is inverse at protonophore concentrations where the uncoupler-induced dark conductivity reaches saturation. Whereas the latter effect is induced by conducting photoproducts that accumulate in the membrane, the former is due to a photoinhibition of CCCP. The accumulation of photoproducts is able to provoke an increase in membrane conductance and membrane rupture (Fig. 12).

Provided that, at low CCCP concentrations, the charged photoproducts are able to leave the membrane and therefore do not significantly contribute to the total conductivity, a simple expression was derived (Eq. 15) that allows three experimentally confirmed predictions:

1. Because O_r is proportional to the intensity of light I, G_{rel} is also expected to depend linearly on I (Fig. 10).
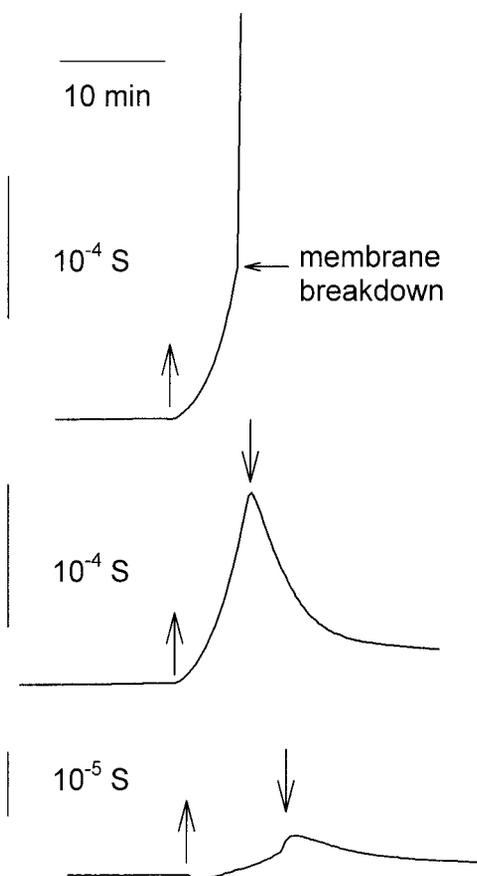

FIGURE 12 The photosensitized increase of CCCP-mediated membrane conductivity. Upward arrows mark the beginning, downward arrows the end of light exposure. The experimental conditions differ from Fig. 3 only in the higher protonophore concentration: (A) In the presence of 100 μM CCCP, light exposure led to membrane breakdown. (B) In another run of this experiment, the membrane was kept from breaking down by a decrease of the illumination time. However, membrane conductivity did not return to baseline. (C) At an aqueous concentration of 20 μM CCCP, an initial decrease of membrane conductivity was followed by its increase. Also under these conditions, membrane conductivity did not return to the level measured in the dark.

2. The flux of fresh CCCP molecules from the aqueous into the organic phase is anticipated to be limited by diffusion across the USL. In the absence of stirring, both the size of the USL and G_{rel} are maximal (Fig. 3).
3. G_{rel} does not depend on the CCCP concentration (Fig. 8).

Due to an interfacial asymmetry in the rate of the photodynamic reaction, a photopotential is generated. A flux of unmodified CCCP molecules is induced along their concentration gradient across the membrane and the USLs. In agreement with the diffusion theory of weak acids and bases (Antonenko et al., 1993, 1997), a pH gradient is generated within the USLs. From a simple mathematical analysis of CCCP diffusion, the photopotential was predicted 1) to be proportional to the light intensity (Fig. 10); 2) to decrease with increasing buffer capacity (Fig. 7); and 3) to increase

with increasing T_b^-, i.e., in parallel to the pH value of the aqueous solution until pH $\gg pK_a$ (Fig. 11), where pK_a is equal to 6.1 (LeBlanc, 1971) and in parallel to the bulk CCCP concentration (Fig. 8).

All predictions were confirmed experimentally. Moreover, the CCCP flux, J, calculated from alterations in membrane conductance, is roughly identical to the one obtained from potential measurements when buffer depletion within the USL is considered (Figs. 8 and 10). Because φ is generated by interfacial differences in the turnover of the photodynamic reaction whereas G reflects the total amount of CCCP damaged, it is concluded that an interleaflet asymmetry in photosensitizer adsorption also generates an asymmetry in the concentration of photoproducts formed. Only a very limited amount of the CCCP anions that are located at the membrane–water interface opposite to the PS serves as a target for the reactive oxygen species formed. The preference of the photodynamic reaction for only one membrane leaflet may have important biological implications, if, for example, changes of the surface potential of only one membrane monolayer are induced.

REFERENCES

Ahmad, N., D. K. Feyes, R. Agarwal, and H. Mukhtar. 1998. Photodynamic therapy results in induction of WAF1/CIP1/P21 leading to cell cycle arrest and apoptosis. *Proc. Natl. Acad. Sci. USA.* 95:6977–6982.

Antonenko, Y. N., G. A. Denisov, and P. Pohl. 1993. Weak acid transport across bilayer lipid membrane in the presence of buffers—theoretical and experimental pH profiles in the unstirred layers. *Biophys. J.* 64:1701–1710.

Antonenko, Y. N., P. Pohl, and G. A. Denisov. 1997. Permeation of ammonia across bilayer lipid membranes studied by ammonium ion selective microelectrodes. *Biophys. J.* 72:2187–2195.

Antonenko, Y. N. and L. Yaguzhinsky. 1982. Generation of potential in lipid bilayer membranes as a result of proton-transfer reactions in the unstirred layers. *J. Bioenerg. Biomembr.* 14:457–465.

Bachor, R., C. R. Shea, R. Gillies, and T. Hasan. 1991. Photosensitized destruction of human bladder carcinoma cells treated with chlorin e6-conjugated microspheres. *Proc. Natl. Acad. Sci. USA.* 88:1580–1584.

Bachowski, G. J., E. Ben-Hur, and A. W. Girotti. 1991. Phthalocyanine-sensitized lipid peroxidation in cell membranes: use of cholesterol and azide as probes of primary photochemistry. *J. Photochem. Photobiol. B.* 9:307–321.

Borisova, M. P., L. N. Ermishkin, E. A. Liberman, A. Y. Silberstein, and E. M. Trofimov. 1974. Mechanism of conductivity of bimolecular lipid membranes in the presence of tetrachlorotrifluormethylbenzimidazole. *J. Membr. Biol.* 18:243–261.

Canti, G., A. Nicolin, R. Cubeddu, P. Taroni, G. Bandieramonte, and G. Valentini. 1998. Antitumor efficacy of the combination of photodynamic therapy and chemotherapy in murine tumors. *Cancer Lett.* 125:39–44.

Chou, P. T., and A. U. Khan. 1983. L-ascorbic acid quenching of singlet delta molecular oxygen in aqueous media: generalized antioxidant property of vitamin C. *Biochem. Biophys. Res. Commun.* 115:932–937.

Diamond, I., S. G. Granelli, A. F. McDonagh, S. Nielson, C. B. Wilson, and R. Jaenicke. 1972. Photodynamic therapy of malignant tumours. *Lancet.* 2:1175–1177.

Ehrenberg, B., J. L. Anderson, and C. S. Foote. 1998. Kinetics and yield of singlet oxygen photosensitized by hypericin in organic and biological media. *Photochem. Photobiol.* 68:135–140.

Girotti, A. W. 1990. Photodynamic lipid peroxidation in biological systems. *Photochem. Photobiol.* 51:497–509.

Gutknecht, J., and D. C. Tosteson. 1973. Diffusion of weak acids across lipid bilayer membranes: effects of chemical reactions in the unstirred layers. *Science.* 182:1258–1261.

Haylett, A. K., F. I. McNair, D. McGarvey, N. F. Dodd, E. Forbes, T. G. Truscott, and J. V. Moore. 1997. Singlet oxygen and superoxide characteristics of a series of novel asymmetric photosensitizers. *Cancer Lett.* 112:233–238.

He, J., C. M. Whitacre, L. Y. Xue, N. A. Berger, and N. L. Oleinick. 1998. Protease activation and cleavage of poly(ADP-ribose) polymerase: an integral part of apoptosis in response to photodynamic treatment. *Cancer Res.* 58:940–946.

Hoebeke, M., H. J. Schuitmaker, L. E. Jannink, T. M. Dubbelman, A. Jakobs, and A. van de Vorst. 1997. Electron spin resonance evidence of the generation of superoxide anion, hydroxyl radical and singlet oxygen during the photohemolysis of human erythrocytes with bacteriochlorin A. *Photochem. Photobiol.* 66:502–508.

Kasianowicz, J., R. Benz, and S. McLaughlin. 1984. The kinetic mechanism by which CCCP (carbonyl cyanide m-chlorophenylhydrazone) transports protons across membranes. *J. Membrane Biol.* 82:179–190.

Kochevar, I. E., J. Bouvier, M. Lynch, and C. W. Lin. 1994. Influence of dye and protein location on photosensitization of the plasma membrane. *Biochim. Biophys. Acta.* 1196:172–180.

Krasnovsky, A. A., Jr.1998. Singlet molecular oxygen in photobiochemical systems: IR phosphorescence studies. *Membr. Cell Biol.* 12:665–690.

Kunz, L. and G. Stark. 1998. Photofrin II sensitized modifications of ion transport across the plasma membrane of an epithelial cell line. II. Analysis at the level of membrane patches. *J. Membrane Biol.* 166:187–196.

Kunz, L., U. Zeidler, K. Haegele, M. Przybylski, and G. Stark. 1995. Photodynamic and radiolytic inactivation of ion channels formed by gramicidin A: oxidation and fragmentation. *Biochemistry.* 34:11895–11903.

Lagorio, M. G., L. E. Dicelio, E. A. San-Roman, and S. E. Braslavsky. 1989. Quantum yield of singlet molecular oxygen sensitization by copper(II) tetracarboxyphthalocyanine. *J. Photochem. Photobiol. B.* 3:615–624.

LeBlanc, O. H. 1971. The effect of uncouplers of oxidative phosphorylation on lipid bilayer membranes: carbonylcyanide m-chlorophenylhydrazone. *J. Membrane Biol.* 4:227–251.

Lee, C., S. S. Wu, and L. B. Chen. 1995. Photosensitization by 3,3'-dihexyloxacarbocyanine iodide: specific disruption of microtubules and inactivation of organelle motility. *Cancer Res.* 55:2063–2069.

Levy, J. G. 1994. Photosensitizers in photodynamic therapy. *Semin. Oncol.* 21:4–10.

Moore, J. V., C. L. West, and C. Whitehurst. 1997. The biology of photodynamic therapy. *Phys. Med. Biol.* 42:913–935.

Mueller, P., D. O. Rudin, H. T. Tien, and W. C. Wescott. 1963. Methods for the formation of single bimolecular lipid membranes in aqueous solution. *J. Phys. Chem.* 67:534–535.

Penning, L. C., and T. M. Dubbelman. 1994. Fundamentals of photodynamic therapy: cellular and biochemical aspects. *Anticancer Drugs.* 5:139–146.

Pohl, P., E. H. Rosenfeld, and R. Millner. 1993. Effects of ultrasound on the steady-state transmembrane pH gradient and the permeability of acetic acid through bilayer lipid membranes. *Biochim. Biophys. Acta.* 1145:279–283.

Pohl, P., S. M. Saparov, and Y. N. Antonenko. 1998. The size of the unstirred layer as a function of the solute diffusion coefficient. *Biophys. J.* 75:1403–1409.

Prinsze, C., T. M. Dubbelman, and J. van Steveninck. 1990. Protein damage, induced by small amounts of photodynamically generated sin-

glet oxygen or hydroxyl radicals. *Biochim. Biophys. Acta.* 1038: 152–157.

Rodgers, M. A. J., and P. T. Snowden. 1982. Lifetime of singlet oxygen in liquid water as determined by time resolved infrared luminescence measurements. *J. Am. Chem. Soc.* 104:5541–5543.

Rokitskaya, T. I., Y. N. Antonenko, and E. A. Kotova. 1993. The interaction of phthalocyanine with planar lipid bilayers—photodynamic inactivation of gramicidin channels. *FEBS Lett.* 329:332–335.

Rokitskaya, T. I., M. Block, Y. N. Antonenko, E. A. Kotova, and P. Pohl. 2000. Photosensitizer binding to lipid bilayers as a precondition for the photoinactivation of membrane channels. *Biophys. J.* 78:2572–2580.

Rosenthal, I. and E. Ben-Hur. 1995. Role of oxygen in the phototoxicity of phthalocyanines. *Int. J. Radiat. Biol.* 67:85–91.

Rywkin, S., L. Lenny, J. Goldstein, N. E. Geacintov, N. H. Margolis, and B. Horowitz. 1992. Importance of type I and type II mechanisms in the photodynamic inactivation of viruses in blood with aluminum phthalocyanine derivatives. *Photochem. Photobiol.* 56:463–469.

Salet, C., G. Moreno, F. Ricchelli, and P. Bernardi. 1997. Singlet oxygen produced by photodynamic action causes inactivation of the mitochondrial permeability transition pore. *J. Biol. Chem.* 272:21938–21943.

Stozhkova, I. N., V. V. Cherny, V. S. Sokolov, and Y. A. Ermakov. 1997. Adsorption of haematoporphyrins on the planar bilayer membrane. *Membr. Cell Biol.* 11:381–399.

Stozhkova, I. N., V. M. Mirsky, R. L. Kayushina, V. V. Erokhin, and A. F. Mironov. 1992. Interaction of hematoporphyrin dimethyl ether with model membrane systems: double bonds of hydrocarbon chains as a target for photodynamic damage of lipid membranes. *Biol. Membrany.* 9:74–79.

Straessle, M., and G. Stark. 1992. Photodynamic inactivation of an ion channel: gramicidin A. *Photochem. Photobiol.* 55:461–463.

Sun, K., and D. C. Mauzerall. 1996. A simple light-driven transmembrane proton pump. *Proc. Natl. Acad. Sci. USA.* 93:10758–10762.

Valenzeno, D. P., and M. Tarr. 1991. Membrane photomodification and its use to study reactive oxygen effects. *In* Photochemistry and Photophysics. J. F. Rabek, editor. CRC Press, Boca Raton, Ann Arbor, Boston. 137–191.

Zang, L. Y., B. R. Misra, K. J. van Kuijk, and H. P. Misra. 1995. EPR studies on the kinetics of quenching singlet oxygen. *Biochem. Mol. Biol. Int.* 37:1187–1195.